U.S. DEPARTMENT OF COMMERCE • John T. Connor, Secretary

ENVIRONMENTAL SCIENCE SERVICES ADMINISTRATION
Robert M. White, Administrator

Weather Bureau

TECHNICAL NOTE 4-NSSL-25

A Comparison of Kinematically Computed Precipitation With Observed Convective Rainfall

James C. Fankhauser

WASHINGTON, D.C.
September 1965

TABLE OF CONTENTS

A COMPARISON OF KINEMATICALLY COMPUTED PRECIPITATION WITH OBSERVED CONVECTIVE RAINFALL

James C. Fankhauser

National Severe Storms Laboratory
Norman, Oklahoma

ABSTRACT

Observed wind and moisture patterns in an extensive squall-line development are used to compute precipitation from a continuity equation for moist air. Horizontal flux of water vapor accounts for about 80 percent of the observed rainfall, and when the local change in water vapor content is included in the moisture balance equation, the computed budget accounts for 95 percent of the actual rainfall production. Factors neglected in the quantitative assessment of the water budget are (1) the transport of water in liquid and solid state and (2) the evaporation from the ground. The results obtained indicate that the agreement between kinematically computed precipitation and observed rainfall improves with the density of rawinsonde observations. Small directional shear in the vertical wind field is proposed as a mechanism for making the squall line an efficient rainfall producer.

1. INTRODUCTION

In recent years numerous synoptic studies have compared the observed rainfall to kinematically computed precipitation using observed winds [1, 10, 12, 15]. Satisfactory agreement has been obtained in investigations of this type when the magnitudes of the vertical motions were significantly large and uniform over a broad region.

Accuracy of kinematical computations of precipitation depends essentially upon the density and quality of wind and moisture observations. For a given storm intensity, increased observational density, and/or frequency, should allow definition of the divergence-precipitation relationship on a scale somewhat smaller than ordinary synoptic. This scale would include the organized convective outbreaks typical of the Plains area in the central United States.

In this paper the precipitation computed from the equation of continuity for moist air is compared to heavy rainfall that occurred in conjunction with the squall-line development of May 28-29, 1962. In defining the wind and moisture fields, optimum use is made of serial rawinsonde ascents requested by the U. S. Weather Bureau's National Severe Storms Project and Severe Local Storms Forecast Center[1]. Details provided by these observations were considered sufficient to allow some quantitative estimates of the water budget involved. The role of vertical directional shear as a possible determining factor in producing locally heavy rainfall is also discussed.

2. SYNOPTIC SITUATION

During the latter part of May 1962 the synoptic situation at the surface featured a large anticyclone covering the eastern one-third of the continental United States, which provided a flow of warm, moist air northward from the Gulf of Mexico. Scattered convective activity had been increasing daily within this sustained supply of maritime tropical air and on the afternoon of May 28 a synoptic-scale squall line erupted in response to the approach of a deep, upper-level cold trough from the west.

Surface conditions in the early hours on this day showed a weak, dry, cold front extending from a low pressure center in southeastern Colorado southward through the Oklahoma and Texas panhandles. During succeeding hours the surface cyclone moved northeastward at a speed of about 15 kt. while the dry front progressed more slowly eastward reaching eastern Kansas and central Oklahoma and Texas by early on the 29th.

Upper-level conditions, represented by the series of 500-mb. charts in figure 1, combined with the available low-level flow of moist air to produce a broad area of potential instability. The lifted index and surface frontal positions are shown on the 850-mb. charts in figure 2.

H. A. Brown [4] has discussed this case in some detail and compared it to the situation of September 29-30, 1954 (see [3, 7, 14]), in which apparently independent, organized mesosystems became aligned in such a manner as to produce a

---

[1]For a resumé of the unusually large quantity of special soundings and radar scope photography available in this case see; Sanders, L. D., "Field Operations of the National Severe Storms Project in Spring 1962," National Severe Storms Project Report No. 14, 1963, U. S. Weather Bureau, Washington, D. C., p. 47.

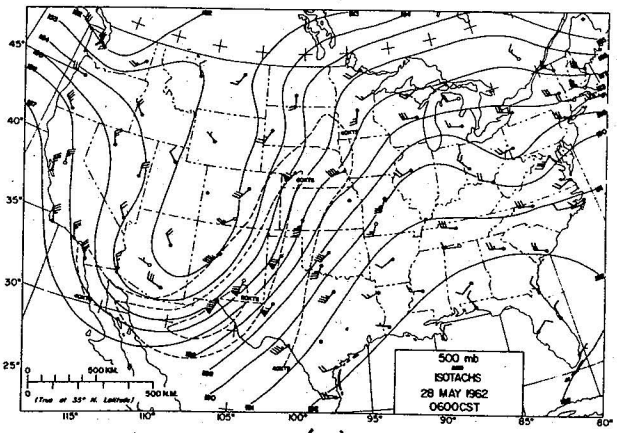

(a)

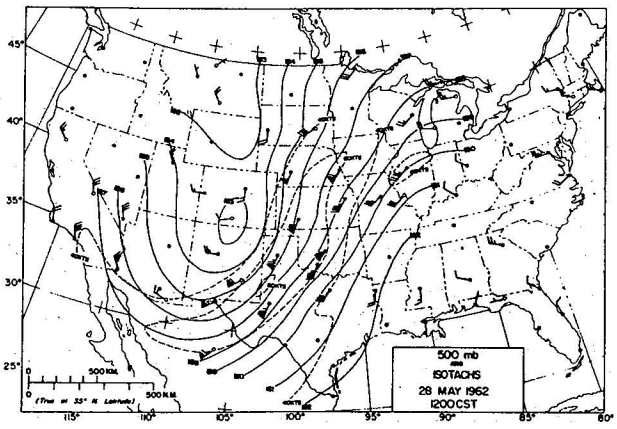

(b)

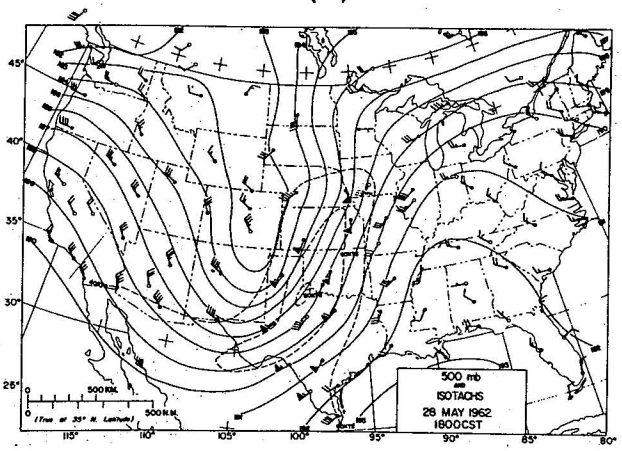

(c)

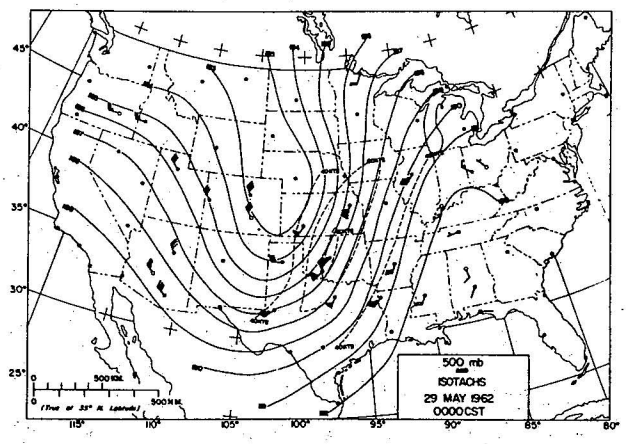

(d)

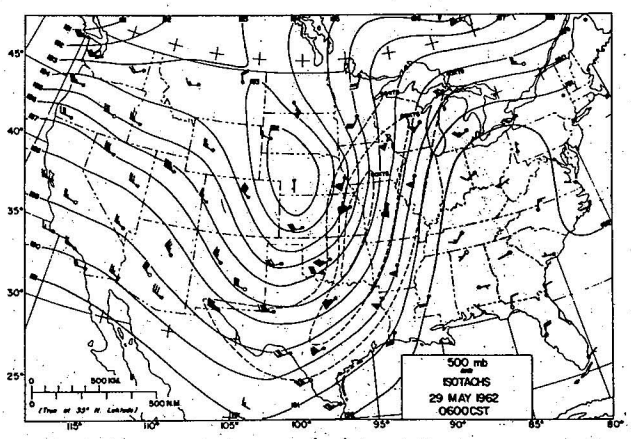

(e)

Figure 1. - 500-mb. contour and isotach analysis, May 28-29, 1962. Solid lines are height contours in hundreds of feet. Dashed lines are isotachs at 20 kt. intervals.

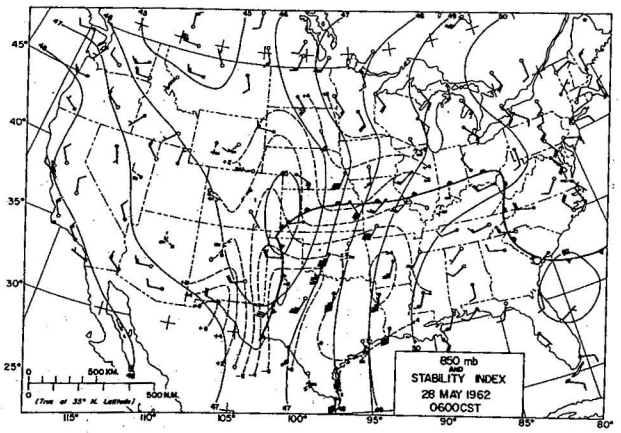

(a)

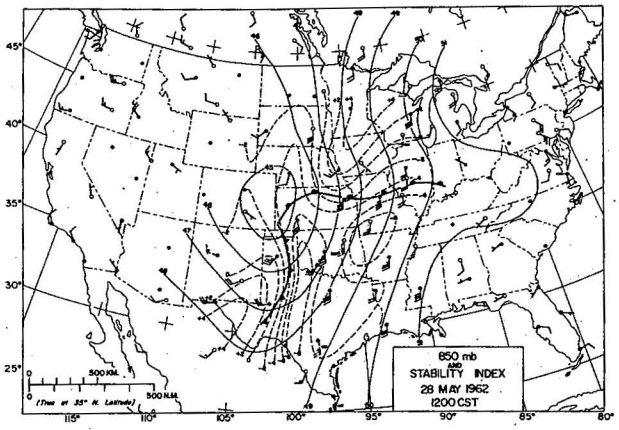

(b)

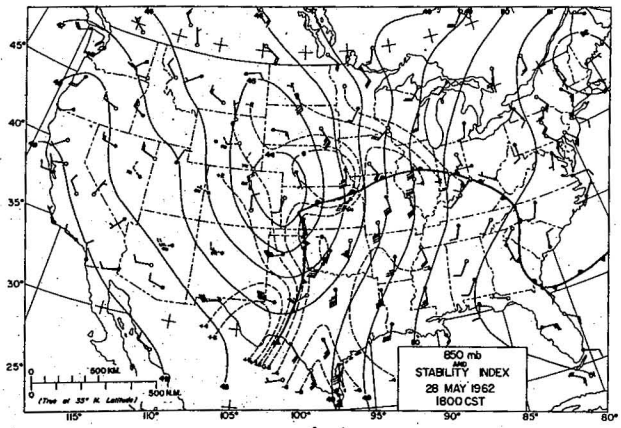

(c)

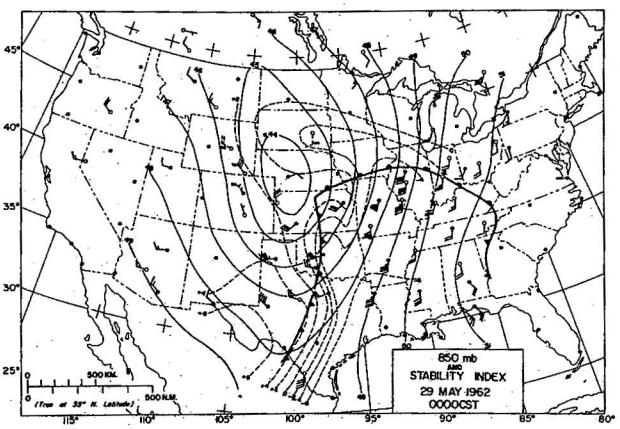

(d)

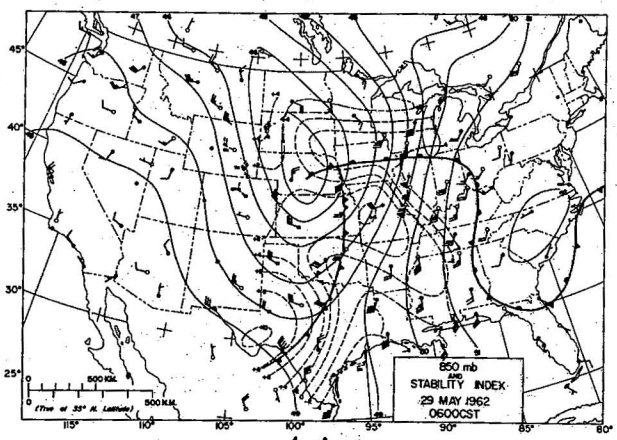

(e)

Figure 2. - 850-mb. contours, surface fronts, and stability analysis, May 28-29, 1962. Solid lines are height contours in hundreds of feet. Dashed lines are isopleths of stability index at intervals of 2°C.

convective zone of nearly macroscale proportions. Development of the resulting squall line can be followed by referring to the radar echo composites in figure 3. At mid-day a conglomerate area of thunderstorms was active near and to the north of the warm front in northeastern Kansas, while to the south the convective activity was similar to that on preceding days with patches of thunderstorms scattered throughout the warm air mass. By mid-afternoon some clusters of these storms became definitely aligned, and at 1800 CST a continuous squall-line zone 600 to 700 n. mi. in length had been established. This zone was maintained in a slowly dissipating state as the line moved eastward into Iowa, Missouri, Arkansas, and northeastern Texas by early on the 29th. Although the convective activity associated with the squall line was not unusually severe, it produced a belt of heavy rainfall that extended from western Iowa into central Texas.

3. CHARACTER AND ANALYSIS OF WIND AND MOISTURE FIELDS

A serious problem affecting the analysis of the upper winds in convective storm situations is the locally disturbed character of individual observations induced by the propinquity of the thunderstorms themselves. An individual thunderstorm sounding frequently displays little continuity when compared to neighboring soundings taken at the regular synoptic spacing.

Through the use of serial rawinsonde ascents at intervals of 6 hr. or less it was possible, in this case, to detect a systematic influence of organized convection which uniformly distorted the character of the broad-scale flow. After being adjusted in time and space with respect to the squall-line motion, the auxiliary observations were incorporated as an aid to determining the streamline analyses that appear in figure 4. Examination of the serial sequences at Topeka, Oklahoma City, Ft. Sill, and Fort Worth, discloses that the disturbance to the wind field results in exaggerated net low-level convergence and upper-level divergence that exceeds the ordinary synoptic values. Each observation in a particular series appears to lend credibility and continuity to the others, and in general the quality and frequency of available observations were accepted as sufficient for defining the instantaneous wind field at 1800 CST. From streamline analyses similar to those presented in figure 4, isotach and isogon patterns were obtained at 50-mb. intervals between the surface and 200 mb.

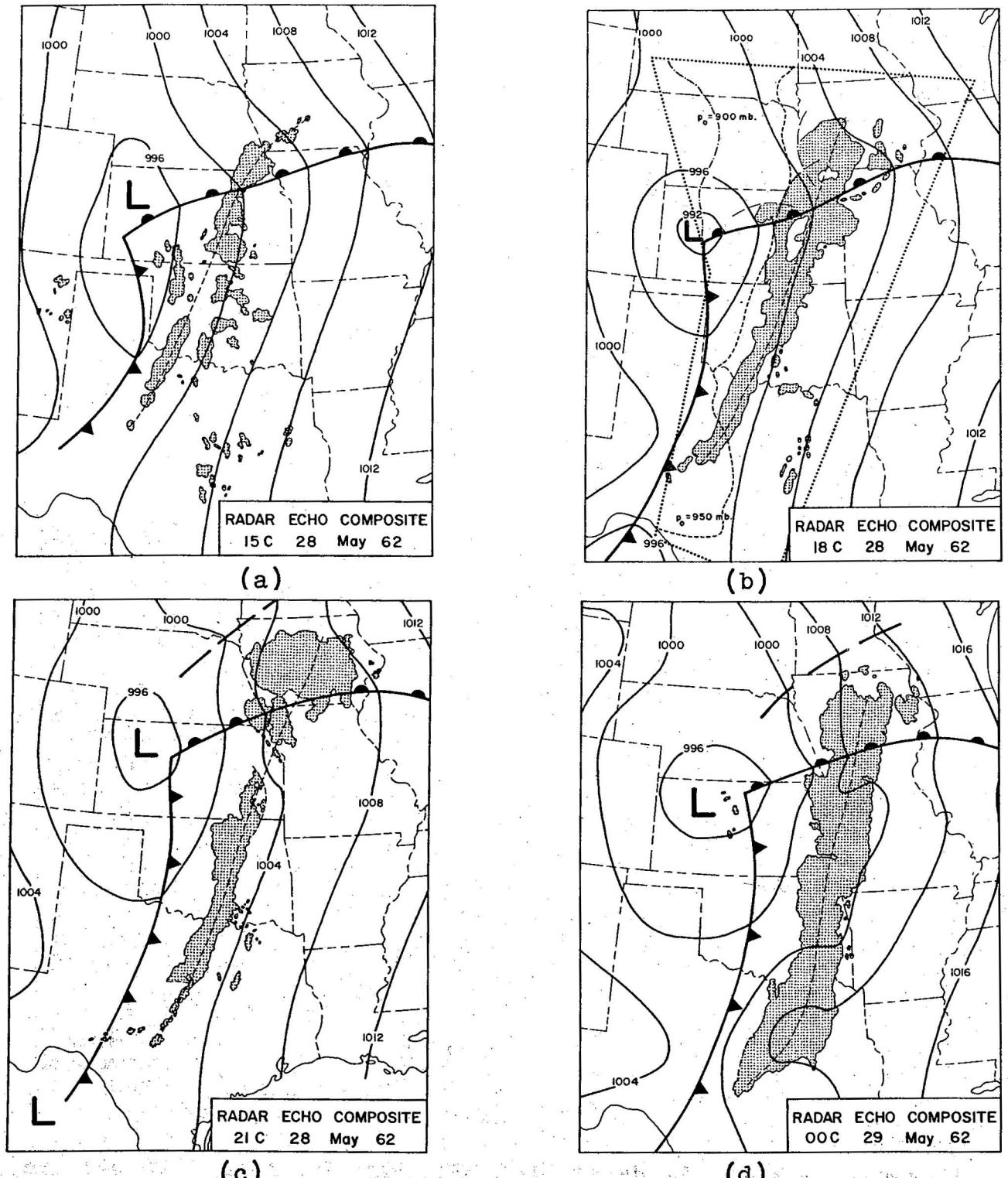

Figure 3. - Composite radar echoes, May 28-29, 1962. Sea-level fronts and isobars taken from NMC analysis. Dotted lines in figure 3b delineate area (A_p = 1.165 x 10^{12} m.^{2}) used for computations discussed in section 5. Dashed and dash-dot contours in left-hand portion of A_p denote surface intercepts of 950-mb. and 900-mb. constant pressure-surfaces.

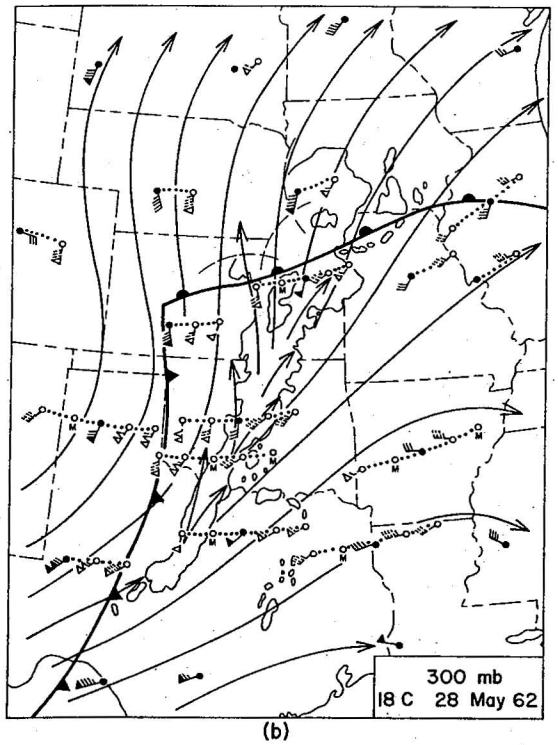

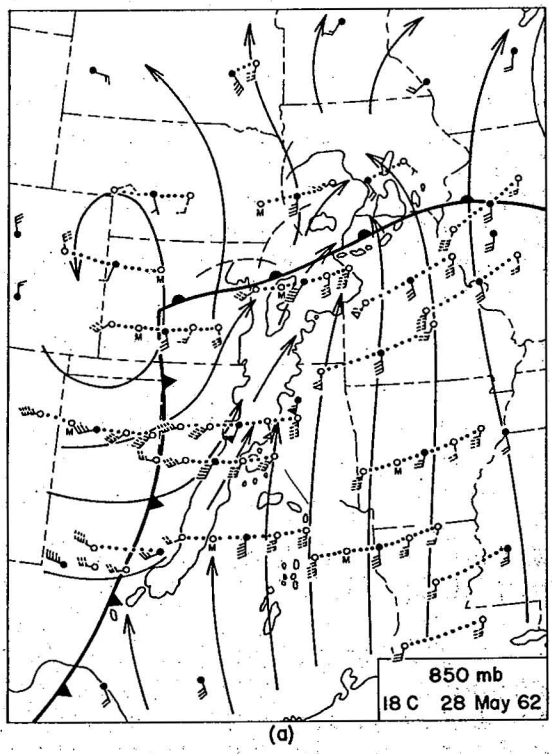

Figure 4. - Wind fields at 1800 CST, May 28, 1962. Arrows are streamlines; irregular thin lines are composite radar echoes; heavy lines, surface fronts. Dashed wind symbols are observations 6 hr. and 3 hr. before (to the right), and 3 and 6 hr. after (to the left) 1800 CST, at stations with solid symbols at map time.

In areas where rapid condensation and precipitation rates were occurring, the details provided by the serial soundings also allowed a seemingly credible evaluation of the horizontal distributions of moisture on a sub-synoptic scale. Values of specific humidity were graphically integrated through layers of 50-mb. thickness and analyzed for all layers from the surface to 300 mb.

4. WATER BUDGET IN CONVECTIVE SYSTEMS

The total budget of moisture in a vertical air column has been partitioned by Väisänen [15] in the following way:

a. The flux of water vapor through the vertical walls and upper boundary;

b. the flux of water in liquid and solid states through these same boundaries;

c. the precipitation from the column; and

d. the evaporation from the ground.

With some assumptions as to the relative importance of these and other possible contributions, a continuity equation for moist air, which relates the precipitation rate P, per unit time and area, to the balance between the local change in water vapor and the items a and d can be stated:

$$P = E - \frac{1}{g} \int_{p}^{p_o} \frac{\partial q}{\partial t} \, dp - \frac{1}{g} \int_{p}^{p_o} \nabla \cdot q \mathbf{V} \, dp \qquad (1)$$

where E is the evaporation from the ground, q the specific humidity, and $\mathbf{V}$ the horizontal wind.

In equation (1) the flux of water in liquid and solid form through the vertical walls and upper boundary is neglected and it is assumed that condensed water immediately precipitates. Palmén and Holopainen [12] have pointed out that the latter condition is not always valid for small regions and in a study by Bradbury [1], in which the computational area was of the synoptic scale, there is some evidence of time lag between computed and observed precipitation that indicates partial storage of liquid water for as long as 12 to 18 hr. The validity of the immediate precipitation of condensed water vapor remains to be tested in the case under study.

Neglect of the transport of water in liquid and solid form through the vertical walls and top of the column is justified in non-convective cases by judicious placement of the vertical boundaries at the edge of the precipitation area. Applying this technique to convective systems may be justified at low levels but near the cloud tops the prodigious "blow-off" that develops in typical wind environments possessing strong vertical directional shear, could transport significant amounts of glaciated cloud material across the upper vertical boundaries. Fujita and Byers [6] present data which show that nearly 50 percent of the cloud contained within the visual boundaries was concentrated in the non-precipitating anvil. Braham [2] points out, however, that even though the outflow aloft is saturated and may contain ice crystals or cloud droplets, relatively little water is likely to be involved in view of the low temperatures at the upper levels. Furthermore, in the case under study the mean tropospheric winds were parallel to the squall-line axis and the vertical directional shear was small, so that portions of cloud mass exported horizontally by outflow aloft should have been aligned along, and contained within, the convective zone. These considerations suggest that the neglect of assumption b is not serious in this special case.

The effect on the moisture budget of evaporation from the ground into the column can be regarded as negligible where sustained precipitation is falling over a broad area. In the case of convection where rainfall is occurring in a relatively concentrated zone, the neglect of the contribution made by evaporation becomes less valid. But, since evaporation is very difficult to determine and presumably of secondary importance compared to the other terms in equation (1), it will not be considered in subsequent discussions.

When precipitation is occurring as a result of uniform upward air motions over a broad area, the water vapor content within the atmospheric column overlying the area can be considered to be at nearly steady state. In determining the moisture budget for concentrated zones of convection, where large variations in the precipitation and condensation rates are likely, the contributions of the local change should, and in this investigation will, be included.

5. MEAN PROFILES OF THE WATER VAPOR TRANSPORT, DIVERGENCE, AND VERTICAL VELOCITY

In order to obtain a gross comparison between the net horizontal flux of water vapor and the observed precipitation an approach similar to that of Palmén [11] is adopted. A boundary of length, L, enclosing the squall line at 1800 CST and encompassing an area, $A_p = 1.165 \times 10^{12}$ m.^{2}, was laid out as shown in figure 3c. The net amount of water vapor transported across the vertical boundaries is expressed by:

$$-\frac{1}{g}\int_{p}^{p_o}\oint_{L} qv_n \, dpdL \qquad (2)$$

where q is the specific humidity, and v_n is the normal component of wind (directed positive outward).

In the practical evaluation of formula (2) the vertical integration of qv_n was performed through layers of thickness $\Delta p = 50$ mb. from horizontal averages taken across increments of 80 to 90 km. It was also considered desirable to take into account the sloping surface of p_o by computing the vertical cross-sectional area ($\Delta L \Delta p$) for the lowest layer around the boundary.

The vertical distributions of the mean divergence, $\bar{D}_p$, and vertical velocity, $\bar{\omega}_p$, for the region, A_p, are computed from the expressions

$$\bar{D}_p = \frac{1}{A_p}\oint v_n \, dL \qquad \text{and} \qquad (3)$$

$$\bar{\omega}_p = \frac{\partial p_o}{\partial t} - \int_{p_o}^{p} \bar{D}_p \, dp \qquad (4)$$

In applying the continuity equation expressed in equation (4) the contribution of the local change in surface pressure ($\partial p_o/\partial t$) is justifiably neglected, since the average over the entire region was only about -0.1 μb.sec.$^{-1}$ (-0.1 microbar sec.$^{-1}$), much less than the change in vertical motion through any of the individual 50-mb. layers over which $\bar{\omega}_p$ was integrated. Variable pressure depth in the lowest layer also dictated special handling in the computation of vertical motion.

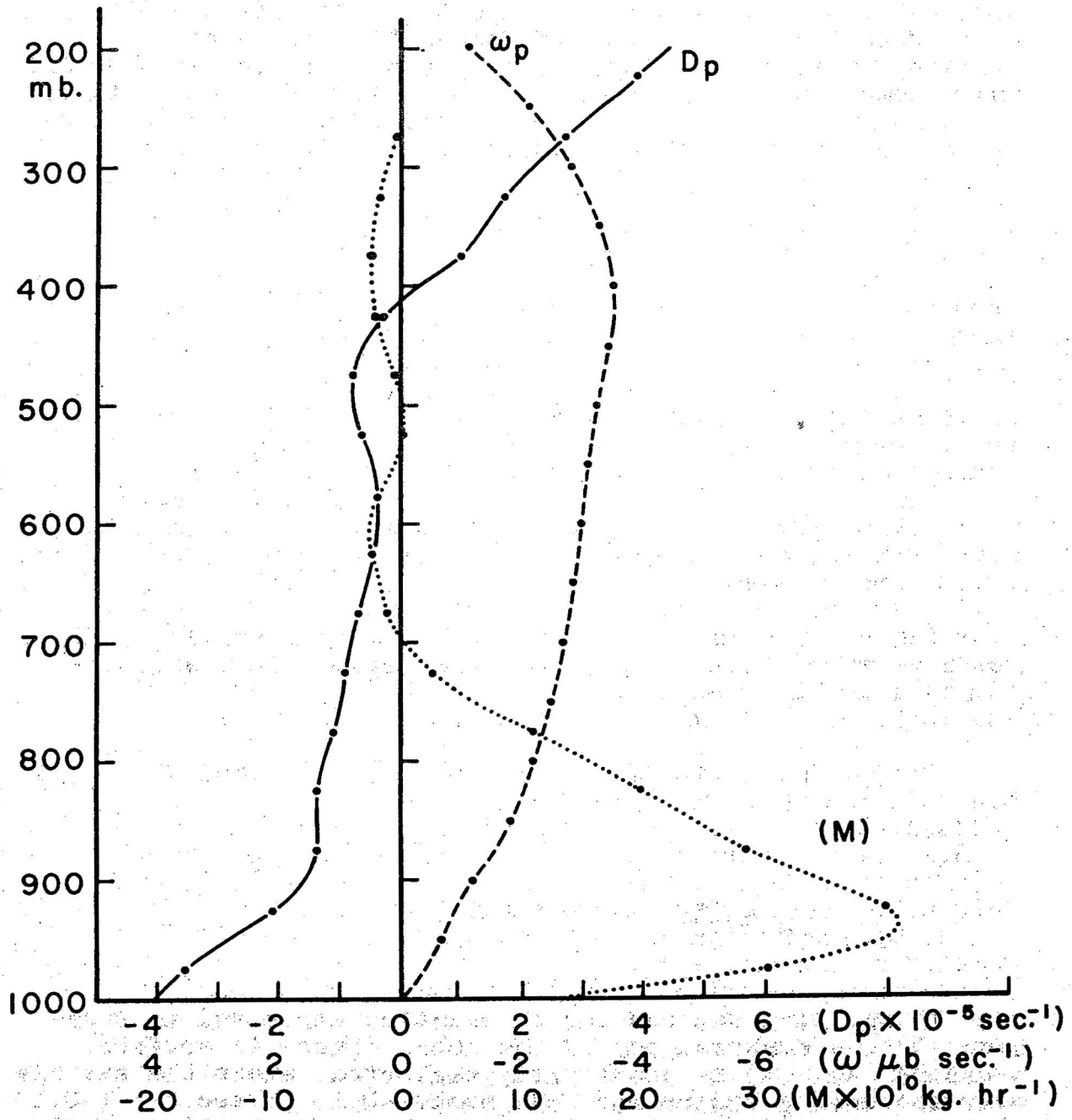

Figure 5. - Mean divergence ($\overline{D}_p$), vertical velocity ($\overline{\omega}_p$), and moisture convergence ($\overline{M}$) profiles for the area, A_p, at 1800 CST.

Evaluation of equations (2), (3), and (4) produced the mean vertical profiles shown in figure 5. Results are similar to those found by Palmén and Holopainen [12] and represent only the general features. The moisture convergence profile demonstrates the combined effects of convergence and high specific humidity values concentrated in the low levels, and is in agreement with the findings of Bradbury [1] that the major moisture transport occurs below about 800 mb.

In order to compare the total water vapor influx to the observed rainfall, isohyets were obtained for the hourly rainfall that occurred within A_p between 1500 CST and 2100 CST. The total mass of the liquid water precipitated during each hourly period was then evaluated through the use of a planimeter. Figure 6a shows the results as a function of time. Cumulative contributions of various precipitation rates toward the total mass are distinguished by shading. Changes in the size of the area over which rainfall occurred are represented by the heavy solid curve. The total mass precipitation rate increased rapidly between the hours of 1500 CST and 1800 CST and compares well with the development of the squall-line zone depicted by the radar composites in figure 3.

The average observed precipitation rate, P , per unit area, for the 6-hr. period amounted to 1.2 mm. $hr.^{-1}$. P as a function of time is represented by the stippled area in figure 6b and the solid straight line denotes the average rate for 6 hr. For comparison, the total influx of water vapor obtained from the evaluation of equation (2) at 1800 CST (1.1 mm. $hr.^{-1}$) is extrapolated across the 6-hr. period and shown as a straight dashed line.

During the 6-hr. period covered in figure 6 a total of 8.4×10^{12} kg. of water was precipitated within A_p . The corresponding release of latent heat of condensation amounts to 5.0×10^{18} calories or 20.9×10^{15} kilojoules; which results in a mean release rate of 96.8×10^{10} kj. $sec.^{-1}$. This value is slightly larger than that found by Palmén and Holopainen (84.1×10^{10} kj. $sec.^{-1}$) near the central part of an intense extratropical cyclone [12]. The difference depends essentially upon the water vapor content of the atmosphere and the intensity of the water vapor flux in each situation. Since the available water vapor was comparable for both cases, the water vapor convergence, or indirectly the magnitude of the vertical motions due to convective processes, very likely accounts for greater release rate in the case discussed here.

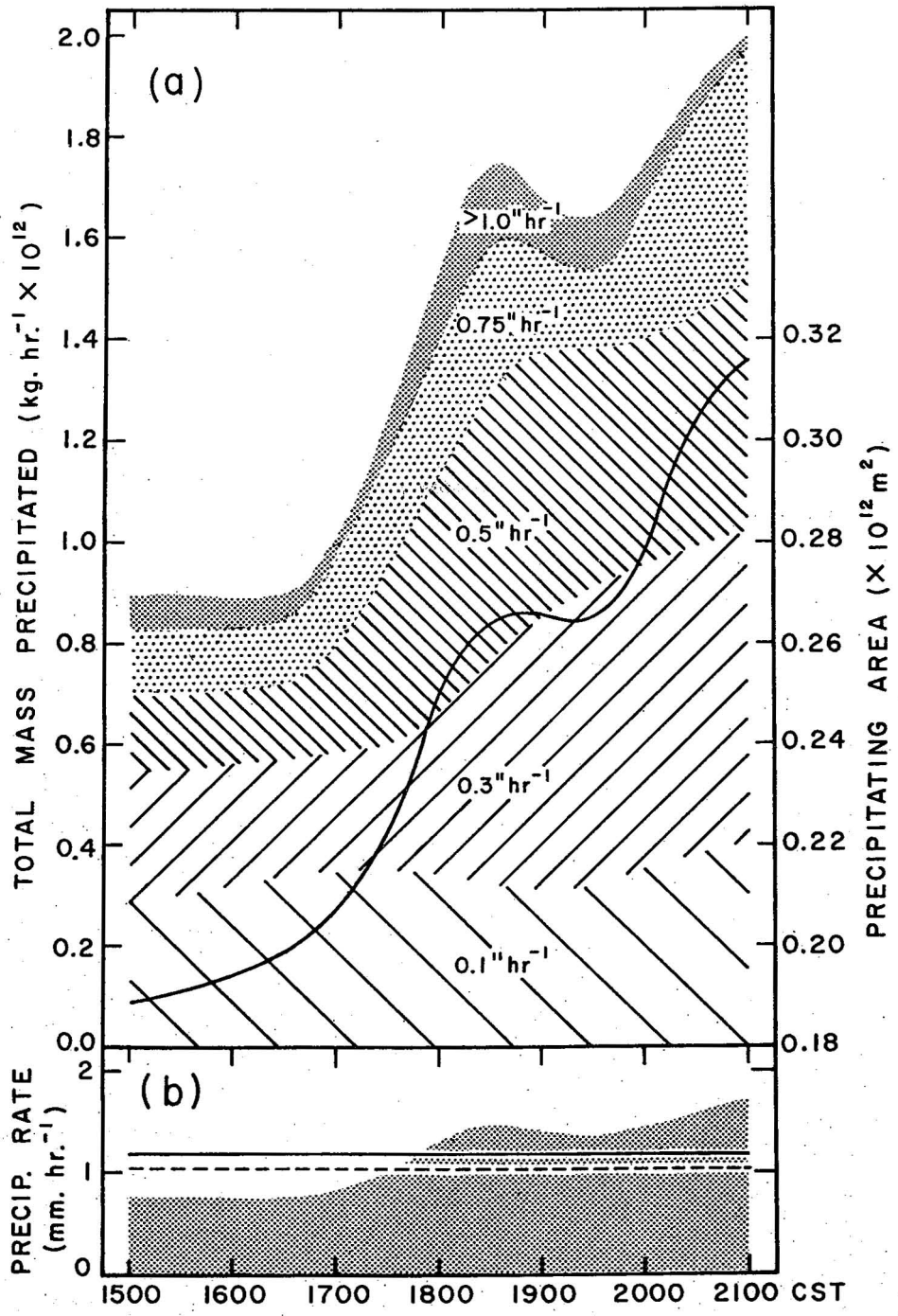

Figure 6. - Precipitation diagram. (a) Total hourly mass precipitation rate into the area A_p as a function of time. Cumulative contributions of various precipitation rates toward the total mass are shown by shading. Heavy curve represents change in the size of the precipitating area. (b) Precipitation rate as a function of time averaged over A_p is shown by stippling. Solid straight line represents rate averaged over 6 hr. Dashed line is rate computed at 1800 CST.

6. NUMERICAL COMPUTATION OF DIVERGENCE, VERTICAL VELOCITY, AND WATER VAPOR FLUX

The results presented in the foregoing section were sufficiently encouraging to suggest the investigation of the horizontal fields of divergence, vertical velocity, and moisture convergence. When the basic equations defining these quantities are expressed in spherical coordinates they take the form:

Divergence: $$\nabla \cdot \mathbf{V} = \frac{1}{a \cos \phi} \left[\frac{\partial u}{\partial \lambda} + \frac{\partial (v \cos \phi)}{\partial \phi}\right] \tag{5}$$

Vertical Velocity: $$\omega_{p_k} = \omega_{p_{k-1}} - \overline{\nabla \cdot \mathbf{V}}\, \Delta p, \quad (\Delta p = 50\text{-mb.}) \tag{6}$$

Moisture Flux: $$M = -\frac{1}{g} \int_{p_k}^{p_{k+1}} \nabla \cdot q\, \mathbf{V}\, dp \tag{7}$$

$$= -\frac{1}{g(a \cos \phi)} \int_{p_k}^{p_{k+1}} \left[\frac{\partial (q\, u)}{\partial \lambda} + \frac{\partial (q\, v \cos \phi)}{\partial \phi}\right] dp$$

where;
- u is the eastward component of velocity,
- v the northward component of velocity,
- q the specific humidity,
- ϕ latitude,
- λ longitude,
- g acceleration of gravity,
- a the mean radius of the earth, and
- p_k denotes the constant pressure levels (k increasing with decreasing pressure)

In order to make the equations tractable for numerical computation they were put into finite difference forms similar to those used by Omoto [10]. Computations were carried out over the geographic area shown in figure 7. A unit grid block with horizontal dimensions of 1.5° latitude and longitude and a vertical increment of 50-mb. pressure depth was adopted and notation used for the identification of grid input and printout locations is shown in the inset. Locators in parenthesis denote points on the pressure surfaces where data were entered and brackets signify the grid block center where printout was obtained.

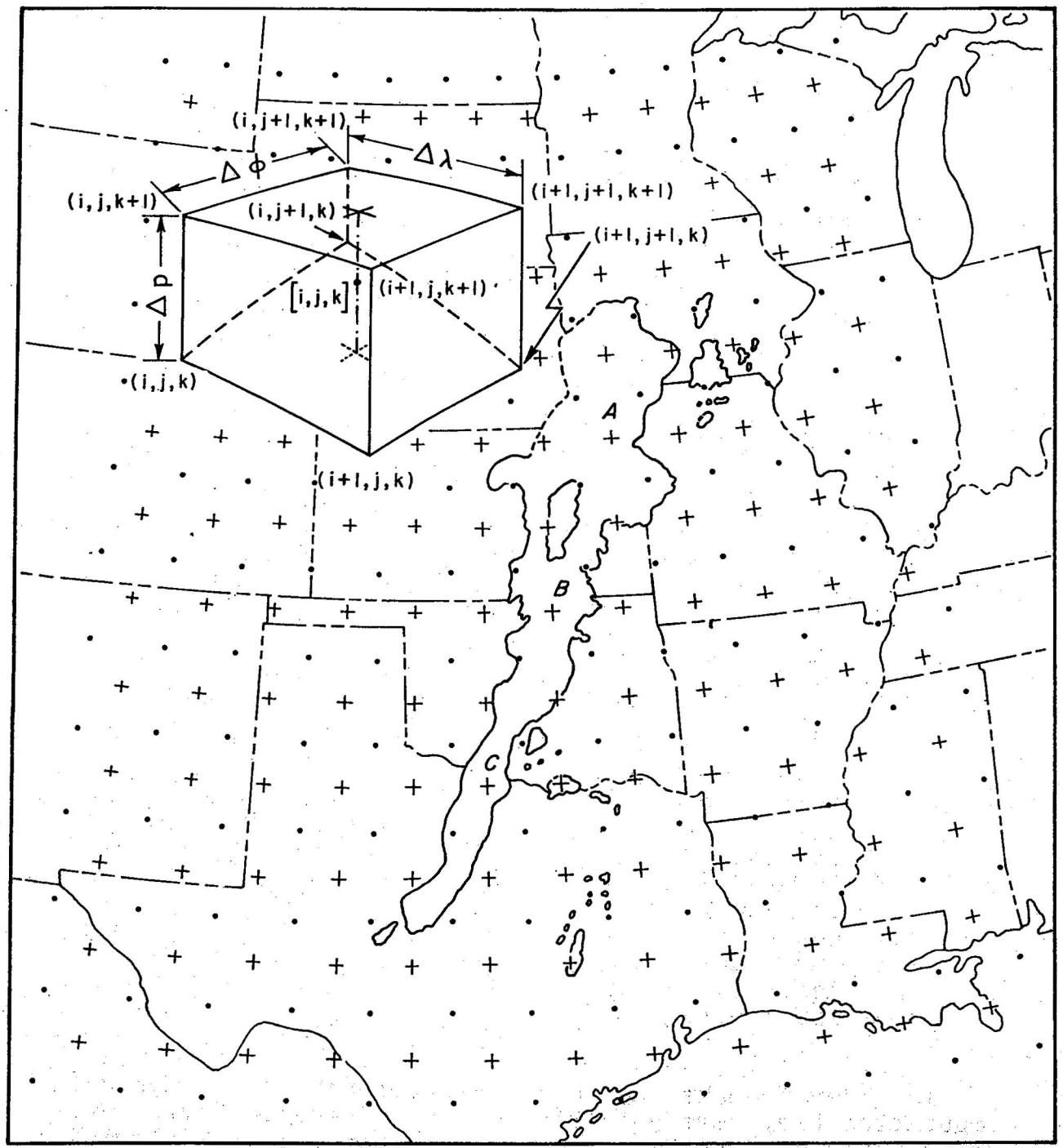

Figure 7. - Grid used for numerical computations; dots and crosses denote input and printout locations respectively. Points labeled A, B, and C, were used to obtain composite vertical profiles shown in figure 9. Inset shows grid element with pressure (p) as vertical coordinate; horizontal coordinates are latitude (ϕ) and longitude (λ). Parenthesis denotes input and brackets signify printout locations.

With the application of these notational conventions the finite difference expression for the mean layer divergence $\overline{D}^{[i,j,k]}$ is taken as:

$$\frac{1}{\Delta p(a\cos\phi)}\left[\frac{\partial(u\Delta p)}{\partial\lambda}+\frac{\partial(v\cos\phi\,\Delta p)}{\partial\phi}\right]$$

$$=\frac{1}{\widetilde{\Delta p}^{[i,j,k]}[a\cos(\phi_{(i,j,k)}+0.75)]}\left(\left\{\left[\frac{(\overline{u}\Delta p)_{(i+1,j+1)}+(\overline{u}\Delta p)_{(i+1,j)}}{2}\right]\right.\right.$$

$$-\left.\left[\frac{(\overline{u}\Delta p)_{(i,j+1)}+(\overline{u}\Delta p)_{(i,j)}}{2}\right]/\Delta\lambda\right\}$$

$$+\left\{\left[\frac{(\overline{v}\cos\phi\,\Delta p)_{(i,j+1)}+(\overline{v}\cos\phi\,\Delta p)_{(i+1,j+1)}}{2}\right]\right.$$

$$\left.\left.-\left[\frac{(\overline{v}\cos\phi\,\Delta p)_{(i,j)}+(\overline{v}\cos\phi\,\Delta p)_{(i+1,j)}}{2}\right]/\Delta\phi\right\}\right)^{[k]} \qquad (8)$$

An average value for a quantity Q through a particular layer [k] is defined as:

$$(\overline{Q})^{[k]}_{(i,j)}=[(Q)_{(i,j,k)}+(Q)_{(i,j,k+1)}]/2 \qquad (9)$$

and the average pressure depth $\widetilde{\Delta p}$ for a grid block is obtained from

$$\widetilde{\Delta p}^{[i,j,k]}=\frac{[(\Delta p)_{(i,j)}+(\Delta p)_{(i+1,j)}+(\Delta p)_{(i,j+1)}+(\Delta p)_{(i+1,j+1)}]^{[k]}}{4} \qquad (10)$$

Equation (8) includes an approximate compensation for the variable surface pressure boundary. The importance of considering the effects of variable pressure depth in the lowest layer can be seen by examining the differential $\frac{\partial(u\Delta p)}{\partial\lambda}$. Expansion by the product rule gives $\Delta p\frac{\partial u}{\partial\lambda} + u\frac{\partial(\Delta p)}{\partial\lambda}$. The contribution of the last term can be appreciable when there are strong wind components normal to the pressure gradient, such as, in this case, along the eastern slopes of the Rocky Mountains.

When the same notation and conventions used in the divergence equation are applied to the expressions for vertical velocity and water vapor flux the finite difference forms become:

$$\omega_{p_{(k)}}^{[i,j]} = \omega_{p_{(k-1)}}^{[i,j]} - (\overline{D\widetilde{\Delta p}})^{[i,j,k-1]} \tag{11}$$

and $M^{[i,j,k]} =$

$$-\frac{1}{g[a\cos(\phi_{(i,j,k)}+0.75)}\Big(\Big\{\Big[\frac{(\overline{qu}\,\Delta p)_{(i+1,j+1)}+(\overline{qu}\,\Delta p)_{(i+1,j)}}{2}\Big]$$

$$-\Big[\frac{(\overline{qu}\,\Delta p)_{(i,j+1)}+(\overline{qu}\,\Delta p)_{(i,j)}}{2}\Big]/\Delta\lambda\Big\}$$

$$+\Big\{\Big[\frac{(\overline{qv}\cos\phi\,\Delta p)_{(i,j+1)}+(\overline{qv}\cos\phi\,\Delta p)_{(i+1,j+1)}}{2}\Big]$$

$$-\Big[\frac{(\overline{qv}\cos\phi\,\Delta p)_{(i,j)}+(\overline{qv}\cos\phi\,\Delta p)_{(i+1,j)}}{2}\Big]/\Delta\phi\Big\}\Big)^{[k]} \tag{12}$$

7. COMPARISON OF NUMERICAL COMPUTATIONS OF DIVERGENCE, VERTICAL VELOCITY, AND WATER VAPOR FLUX WITH OBSERVED PRECIPITATION

Analyses of the horizontal fields of divergence, vertical velocity, moisture flux, and observed precipitation are presented in figure 8. According to the data, the layer of maximum low-level convergence occurs near the squall line between 850 and 750 mb. Values of convergence larger than -4×10^{-5} sec.$^{-1}$ are depicted as shaded areas in figure 8a. This value is slightly greater than that defined by Petterssen [13] as "intense synoptic." The zone of maximum convergence is concentrated in an area that coincides remarkably well with the position of radar echoes shown in figure 3c. In the area of northeastern Kansas where the heaviest rainfall occurred the convergence reaches the sub-synoptic level of -10^{-4} sec.$^{-1}$. An orographic influence is evident near the Black Hills region, while very strong positive divergence prevails along the eastern slopes of the mountains in Colorado and New Mexico. A small area of convergence, reflecting the dynamic influence of the surface cyclone, appears in western Kansas.

In the vicinity of the squall line, maximum upward vertical velocity occurs near the 600-mb. level. Upward motions greater than -5 μb. sec.$^{-1}$ ($\approx$ 6 cm. sec.$^{-1}$) are designated by the shading in figure 8b. Circulations associated with the cyclone over eastern Colorado appear to produce a synoptic-scale vertical motion field which extends from the low pressure center southeastward into the lower Mississippi River Valley. Superimposed upon the broad uniform field are intense small-scale upward motions within the convective zone which reach magnitudes of up to 30 cm. sec.$^{-1}$. This value may be compared to the strongest kinematic vertical velocity (12 cm. sec.$^{-1}$) found by Reed and Prantner [14] over a squall line at peak development. The strong subsidence along the western edge of the region is apparently a result of complementary orographic and dynamic effects.

Analysis of the total water vapor convergence for all layers from the surface to 300 mb. is shown in figure 8c. A conversion from mass transport to precipitation rate was made by using the close relationship; 1 kg. m.$^{-2}$ hr.$^{-1}$ $\approx$ 1 mm. hr.$^{-1}$. For the purpose of comparison the isohyets derived from the observed, hourly, time-averaged precipitation rate for the period 1700-1900 CST are presented in figure 8d.

With regard to the alignment and location of main features, the agreement between the computed water vapor flux and observed precipitation is in general quite good. Areal distribution of the computed maximum at the north end of the squall line is well correlated with the observed rainfall; however, the secondary maxima in Oklahoma and Texas are displaced slightly southward in

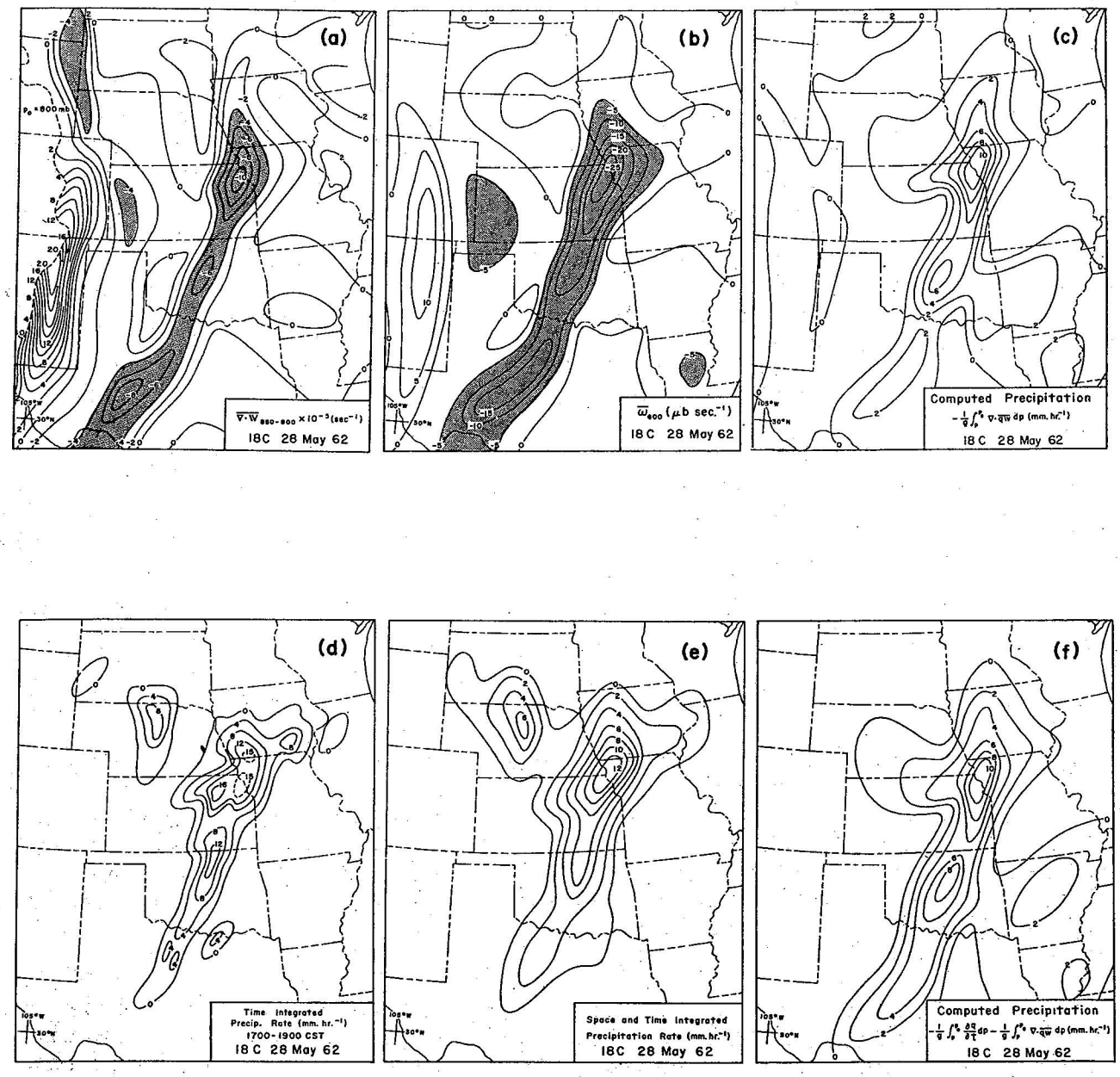

Figure 8. - Analysis for 1800 CST, May 28, 1962 of (a) mean horizontal divergence between 850 and 800 mb. in units 10^{-5} sec.$^{-1}$; (b) vertical velocity at 600 mb. in ub. sec.$^{-1}$; (c) precipitation computed from water vapor convergence (mm. hr.$^{-1}$); (d) observed, time-integrated precipitation rate (mm. hr.$^{-1}$) for period 1700-1900 CST; (e) time-and-space-integrated precipitation rate (mm. hr.$^{-1}$) and (f) precipitation computed from the sum of the water vapor convergence and local change in specific humidity (mm. hr.$^{-1}$).

comparison to the observed centers in those regions. At a smaller time scale, the lag, described by Bradbury [1] and quoted earlier, could well have played a role in this displacement. This is feasible since the individual thunderstorms comprising the line possessed a large component of motion from south to north along the axis of the line [5].

The intensity of water vapor convergence accounts for only about 50 percent of the time-integrated precipitation. However, when the actual rainfall is averaged over space, as well as time, the agreement improves considerably. Figure 8e shows the pattern resulting from the space integration of the isohyets in figure 8d, where averages are taken over grid areas equal to those used in the computation of moisture flux. A comparison now shows that computed values account for 80 percent of the observed rainfall.

Through the use of serial rawinsonde observations at stations near the squall line it was possible to evaluate the local change in water vapor content on a time scale ($\Delta t \leq 6$ hr.) much smaller than is usually possible. The field of the integral,

$$-\frac{1}{g}\int_{200}^{p_o} \frac{\partial q}{\partial t}\, dp \qquad (13)$$

added graphically to the pattern in figure 8c, produces the configuration that appears in figure 8f. Addition of the local change term nearly doubles the computed precipitation at the southern end of the line but makes a progressively smaller contribution northward through the convective zone. Positive contributions as large as 4 mm. hr.$^{-1}$ occur in the central Oklahoma area.

The computed precipitation that appears over Arkansas and Louisiana in figure 8c is not substantiated by observed rainfall. In figure 8f these areas are diminished somewhat by the consideration of local change but there remain unverified computed precipitation areas of significant size and magnitude. This is attributed in part to inadequacies of the data. However, a partial explanation of the discrepancy is also provided by the expanded form of the moisture convergence term in equation (1):

$$-\frac{1}{g}\int_{p_k}^{p_{k-1}} \nabla\cdot q\,\mathbb{V}\, dp = \frac{1}{g}\int_{p_k}^{p_{k-1}} \mathbb{V}\cdot\nabla\, q\, dp - \frac{1}{g}\int_{p_k}^{p_{k-1}} q\,\nabla\cdot\mathbb{V}\, dp \qquad (14)$$

Examination of the analysis of the specific humidity showed that the first term on the right makes the major positive contribution toward the computed precipitation over the area in question.[2] Weak broad-scale upward motions exist over the region and an examination of surface weather charts indicates that cloud cover increased steadily during the period of computation. There is an indication therefore that the converging moisture was being utilized in the production of cloud droplets which were stored aloft rather than released immediately as precipitation.

When this region over the lower Mississippi Valley is neglected, a comparison of the sum of the total moisture convergence and local change terms with the observed precipitation reveals that the computed quantities account for 95 percent of the observed rainfall within the squall-line zone.

In order to obtain a generalized impression of the vertical distribution of divergence and vertical velocity within the convective zone a mean profile for each quantity was derived from the average of computed values obtained at grid points designated A, B, and C in figure 7. The composite profiles are shown in figure 9.

Since upward motions are expected to work to high levels in individual convective towers which reach heights of 40,000 to 50,000 ft., the profiles appear to be unrealistic with regard to the strong subsidence beginning at about 300 mb. Failure of the kinematic method to produce feasible vertical motions at high levels may be due in part to the large grid spacing. When averages are taken over a large region containing thunderstorms, the intense upward motions tend to be compensated for by vigorous downdrafts of comparable magnitude. A net upward motion is to be expected, however, when the convection is near maximum intensity and discrepancies in the vertical motion profile must be attributed to errors in the analysis of the high-level winds or to inherent errors in the winds themselves. Because of computation procedures the accuracy of wind observations decreases with height and errors tend to accumulate and magnify when the observations are used in the integration, since they affect layers of greater linear thickness.

---

[2]This is at variance with findings of Palmén and Holopainen [12] where the last term is shown to account for nearly 85 percent of the total water vapor flux.

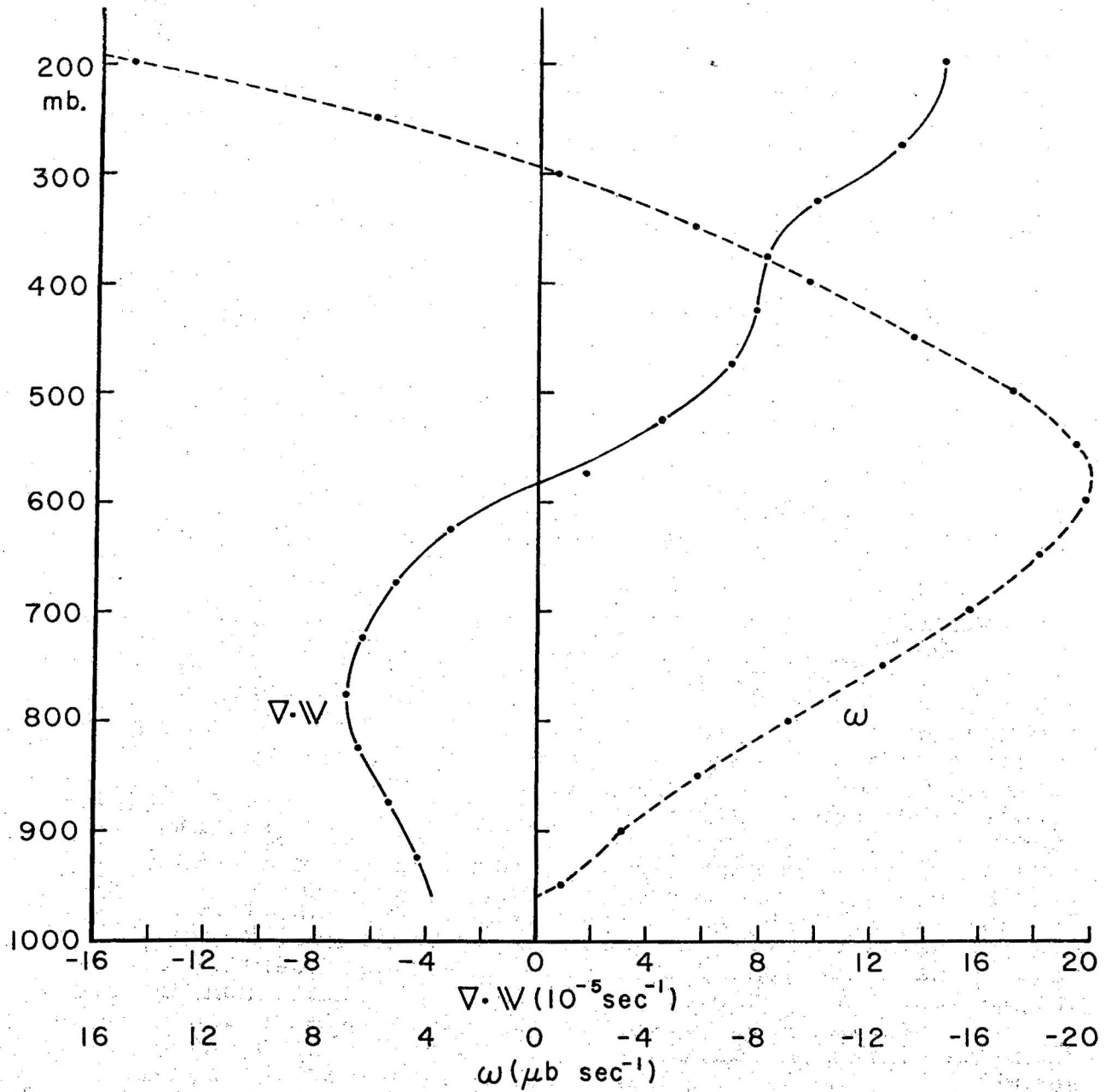

Figure 9. - Mean convective-zone divergence and vertical velocity profiles derived from an average of the computed values at points A, B, and C, in figure 7.

A few remarks about the subjectivity involved in the wind and moisture analyses may be pertinent. Before the analysis was undertaken the analyst was naturally aware of the location and intensity of rainfall areas as well as the distribution of radar echoes which defined the main convective zone. The remarkably good results obtained in comparing computed water vapor flux with the squall-line rainfall may suggest a prejudiced analysis because of the knowledge of rainfall concentrations. An objective approach to the analysis may be substantiated, however, by pointing out that the analyst was equally cognizant of the heavy precipitation area in north-central Nebraska. The computed results in that region failed to account even vaguely for the observed rainfall. The point is that the quality of the computed results appears to be directly related to the amount of detail provided by supplementary observations. Special upper-air soundings were plentiful in the vicinity of the main convective zone but were infrequent and of poor quality in the regions where computations are doubtful or difficult to reconcile with the observed conditions.

8. CHARACTER OF SHEAR AS A CONTRIBUTING FACTOR IN PRODUCING LOCALLY HEAVY RAINFALL

The dynamic efficiency of a convective system as a rainfall producer must be due mainly to the supply of available water vapor and the magnitudes of the vertical motions involved. Newton and Newton [9] have asserted the importance of large directional shear in producing and maintaining updrafts, and Newton and Fankhauser [8] have discussed the relationship between shear and individual storm water-budget requirements.

In addition to the dynamical processes relevant to rainstorm efficiency, a mechanical process inherent in unique vertical shear situations may play a role in producing heavy precipitation over a point. A "squall-line zone" may consist of a single line of radar echoes or may be characterized by a continually evolving multiple line structure. Movement of individual line elements usually differs considerably from the motion of the axis of the line. Individual thunderstorms, in the case discussed here, were found to move on the average along the direction of the mean tropospheric wind which possessed only a small component acting normal to the squall-line axis [5]. As a result there is a large component of storm motion along the line and relatively slow eastward displacement of the convective zone as a whole.

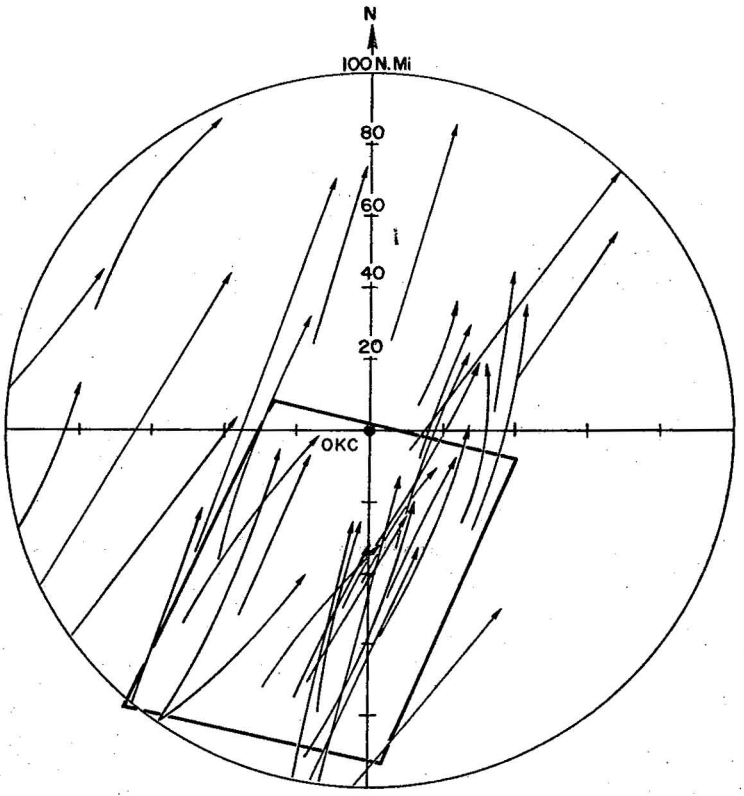

Figure 10. - Radar echo tracks during afternoon and evening of May 28, 1962, within 100 n. mi. of Oklahoma City radar. NSSP Beta Network is shown by the heavy border.

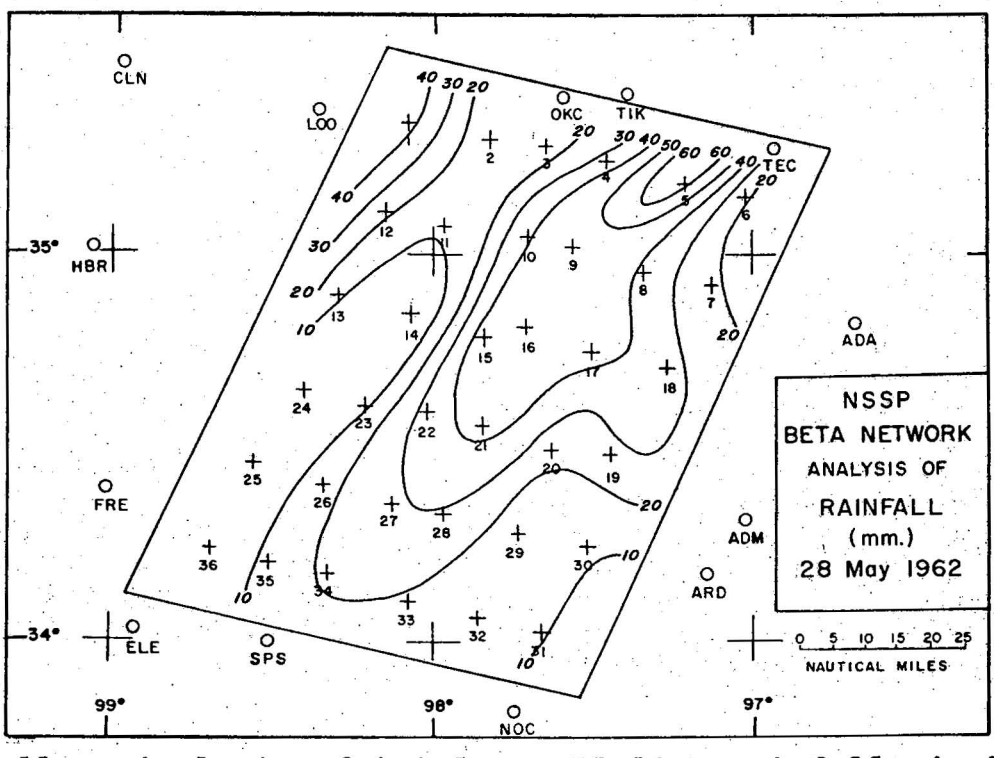

Figure 11. - Analysis of total squall-line rainfall; isohyets at 10 mm. intervals.

The above conditions allow recurrent passage of individual thunderstorms over a particular point beneath the squall line. This phenomenon is portrayed by the radar echo tracks that appear in figure 10. It should be pointed out that, as a result of the restrictions adopted regarding duration and intensity, not all storm tracks are presented; and for those shown, the trajectories represent only the paths of the radar echo centroids. Absence of echo tracks in the vicinity of the radar is a result of histories being interrupted by ground clutter masking. Typical storm size ranged between 8 and 12 n. mi. in diameter at the 21-db. level of attenuation, indicating that the precipitation swaths of many storms were capable of producing frequent periods of rain over the same point.

Analysis of total storm rainfall over the NSSP Beta network is shown in figure 11. The coincidence between the belt of maximum rainfall and the concentration of storm paths in figure 10 supports the premise that the rain-producing potential of a squall line increases when the individual line elements have a large component of motion along the axis of the line.

In this case the motions of the elements comprising the squall line as well as the line itself have been shown to be related in a systematic way to the mean wind through the cloud-bearing layer [5]. Since the mean wind was oriented nearly along the line axis and the directional shear was small, it is suggestive that cases possessing little shear are capable of producing heavier rainfall over a point. It remains, of course, to compare the rain-producing efficiency of squall lines which have developed in comparable air masses but under varying degrees of shear in order to firmly establish the dependence of total rainfall over a point upon shear conditions.

9. SUMMARY AND CONCLUSIONS

In this study it is shown that a continuity equation for moist air, which neglects the horizontal transport of water in liquid and solid form as well as the evaporation from the ground, and give a satisfactory account of the magnitude and areal distribution of space-and-time averaged convective precipitation. Water vapor influx alone accounts for about 80 percent of the observed rainfall, and when the local change in water vapor content is included in the total water budget the computed precipitation amounts to 95 percent of the observed. The assumption that condensed water vapor immediately precipitates does not appear to be critical if computations are performed on a scale significantly larger than an individual convective circulation.

Results indicate that the reliability of the precipitation-divergence relationship for the convective case is highly dependent upon the availability of special upper-air soundings, since the quality of computations is proportional to the frequency of serial rawinsonde observations. These supplementary soundings are also useful in defining the small degree of vertical wind directional shear, which appears to contribute to the overall efficiency of the squall line as a rainfall producer.

From the results presented here, there is an implication that, with an increased density in the rawinsonde network, kinematical computations of precipitation could be used routinely to delineate general areas of heavy convective rainfall, and serve as a valuable tool for the hydrologic forecaster, who is often faced with the responsibility of issuing short-term flood warnings based on frequently delayed and sparse rain-gage reports.

ACKNOWLEDGMENTS

Research reported in this paper was begun while the author was with the National Severe Storms Project, Kansas City, Mo. (Director: Mr. C. F. Van Thullenar) and completed during temporary assignment to the National Center for Atmospheric Research, Boulder, Colo.

Appreciation is expressed for the use of the NCAR Computer Facility and for helpful criticisms and suggestions made by numerous individuals on the staff of NCAR's Dynamical Aspects of Atmospheric Circulation and Synoptic Meteorology Sections. In particular the author wishes to express his gratitude to Dr. C. W. Newton for his stimulation and guidance throughout this investigation. Much enlightenment was also derived from discussions with Prof. E. Palmén and Dr. Y. Omoto during their visits at NCAR.

Thanks are due Mr. Bernard O'Lear for writing the computer program and to Mr. Ralph Coleman for preparing most of the drawings. Mr. Dennis Tussey helped in the plotting and tabulation of raw data.

REFERENCES

1. Bradbury, D. L., "Moisture Analysis and Water Budget in Three Different Types of Storms," Journal of Meteorology, vol. 14, No. 6, December 1957, pp. 559-565.

2. Braham, R. R., Jr., "The Water and Energy Budgets of the Thunderstorm and Their Relation to Thunderstorm Development," Journal of Meteorology, vol. 9, No. 4, August 1952, pp. 227-242.

3. Brown, H. A., "Analysis of a Squall Line: A Line Series of Mesosystems in Different Stages of Development," Technical Report No. 2, U. S. Weather Bureau, Washington, D. C., 1958.

4. Brown, H. A., "On the Low-Level Structure of a Squall Line," Research Paper No. 21, Mesometeorology Project, Department of Geophysical Sciences, University of Chicago, 1963, 19 pp.

5. Fankhauser, J. C., "On the Motion and Predictability of Convective Systems," National Severe Storms Project Report No. 21, 1964 (pre-printed report), 36 pp.

6. Fujita, T., and H. R. Byers, "Model of a Hail Cloud as Revealed by Photogrammetric Analysis," Nubila, vol. 5, 1962,.pp. 85-105.

7. Ligda, M. G. H., "Study of the Synoptic Application of Weather Radar Data," Final Report, Contract AF 19(604)-573, A.and M. College of Texas, 1956, 102 pp.

8. Newton, C. W.,and J. C. Fankhauser, "On the Movements of Convective Storms, with Emphasis on Size Discrimination in Relation to Water-Budget Requirements," Journal of Applied Meteorology, vol. 3, No. 5, December 1964, pp. 651-668.

9. Newton, C. W., and H. R. Newton, "Dynamical Interactions between Large Convective Clouds and Environment with Vertical Shear," Journal of Meteorology, vol. 16, No. 5, October 1959, pp. 483-496.

10. Omoto, Y., "An Investigation of Pre-frontal Precipitation Zones," Scientific Report No. 12, Contract AF 19(604)-7230, Weather Forecasting Research Center, Department of Geophysical Sciences, University of Chicago, 1963, 80 pp.

11. Palmén, E., "Vertical Circulation and Release of Kinetic Energy during the Development of Hurricane Hazel into an Extratropical Storm," Tellus, vol. 10, No. 1, February 1958, pp. 1-23.

12. Palmén, E., and E. O. Holopainen, "Divergence, Vertical Velocity and Conversion between Potential and Kinetic Energy in an Extratropical Disturbance," Geophysica, vol. 8, No. 2, 1962, pp. 89-113.

13. Petterssen, S., Weather Analysis and Forecasting (2d Ed.), McGraw-Hill Book Co., Inc., New York, vol. 1, 1956, p. 293.

14. Reed, R. J., and G. D. Prantner, "A Study of Squall Line Formation in Two Cases," Scientific Report No. 1, Contract AF 19(604)-5192, University of Washington, 1961, 82 pp.

15. Väisänen, A., "Investigation of the Vertical Air Movement and Related Phenomena in Selected Synoptic Situations," Commentationes Physico-Mathematicae, Societas Scientiarum Fennica, XXVI 7, 1961, 72 pp.